

Supporting Information

^{129}Xe NMR-Protein Sensor Reveals Cellular Ribose Concentration

Serge D. Zemerov,^{1,‡} Benjamin W. Roose,^{1,‡} Kelsey L. Farenhem,^{1,‡} Zhuangyu Zhao,¹ Madison A. Stringer,¹ Aaron R. Goldman,² David W. Speicher,^{2,3} and Ivan J. Dmochowski^{1,*}

¹ Department of Chemistry, University of Pennsylvania, Philadelphia, PA 19104, USA.

² Proteomics and Metabolomics Facility and ³ Molecular and Cellular Oncogenesis Program, The Wistar Institute, Philadelphia, PA 19104, USA.

Table of Contents

Table S1. Oligonucleotide primers used for RBP(L19A) insert amplification.....	2
Table S2. Oligonucleotide primers used in RBP site-directed mutagenesis.....	2
Figure S1. SDS-PAGE gel of purified GFP-RBP(L19A).....	2
Figure S2. ITC enthalpograms for ribose binding	3
Figure S3. CD spectra of GFP-RBP(L19A) and mutants	4
Figure S4. Hyper-CEST z-spectra of 10 μM GFP-RBP(L19A) in PBS	5
Figure S5. Hyper-CEST z-spectra of GFP-RBP(L19A) in FBS and serum-free medium.....	6
Figure S6. LC-MS response of [$\text{U-}^{13}\text{C}_5$] ribose spiked into extracted HeLa cell lysate samples	7
Figure S7. Hyper-CEST z-spectra of GFP-RBP(L19A) in FBS-supplemented HeLa cell lysate	8
Figure S8. Ribose calibration curve for LC-MS analysis	9
Table S3. Peak areas and calculated ribose concentrations from LC-MS analysis	10
Figure S9. Time dependent saturation curves with GFP-RBP(L19A).....	11
Figure S10. Saturation contrast as a function of ribose-bound RBP	12
Figure S11. Hyper-CEST z-spectra of RBP mutants.....	13
References.....	14

Table S1. Oligonucleotide primers used for RBP(L19A) insert amplification.

Forward primer	5' – TACTTCCAATCCAATGCAAAAGATACCATCGCGCTGGTCG – 3'
Reverse primer	5' – TTATCCACTTCCAATGTTATTACTGTTTGACAACCAGTTTCAGG – 3'

Table S2. Oligonucleotide primers used in RBP site-directed mutagenesis.

Q235A	Forward primer	5' – GCGACGATTGCAGCGCTGCCGGACCAG – 3'
	Reverse primer	5' – CTGGTCCGGCAGCGCTGCAATCGTCGC – 3'
T135A	Forward primer	5' – GGTATCGCGGGTGCCAGCGCTGCGCGC – 3'
	Reverse primer	5' – GCGCGCAGCGCTGGCACCCGCGATACC – 3'

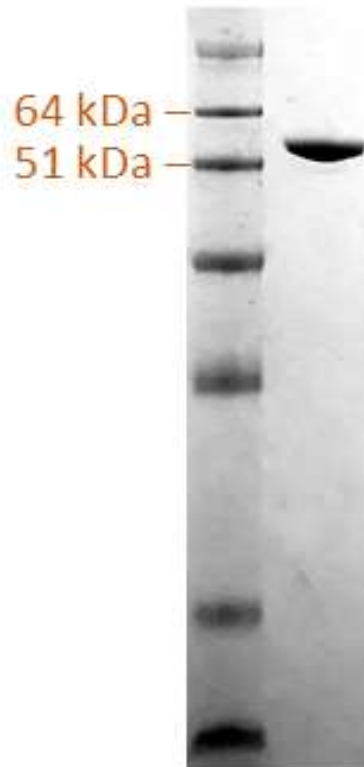


Figure S1. SDS-PAGE gel of purified GFP-RBP(L19A).

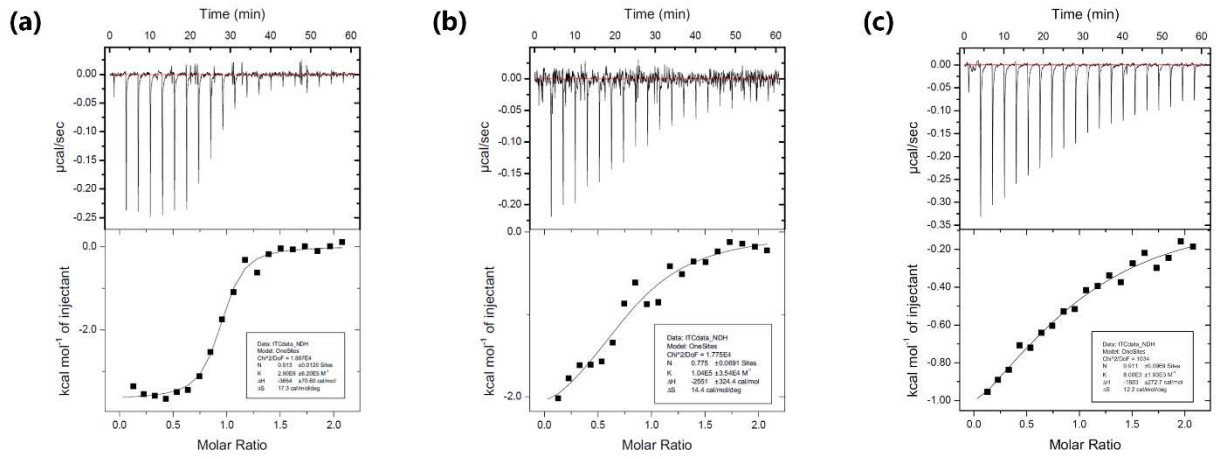


Figure S2. ITC enthalpograms for ribose binding for (a) GFP-RBP(L19A); (b) GFP-RBP(L19A/Q235A); (c) GFP-RBP(L19A/T135A/Q235A).

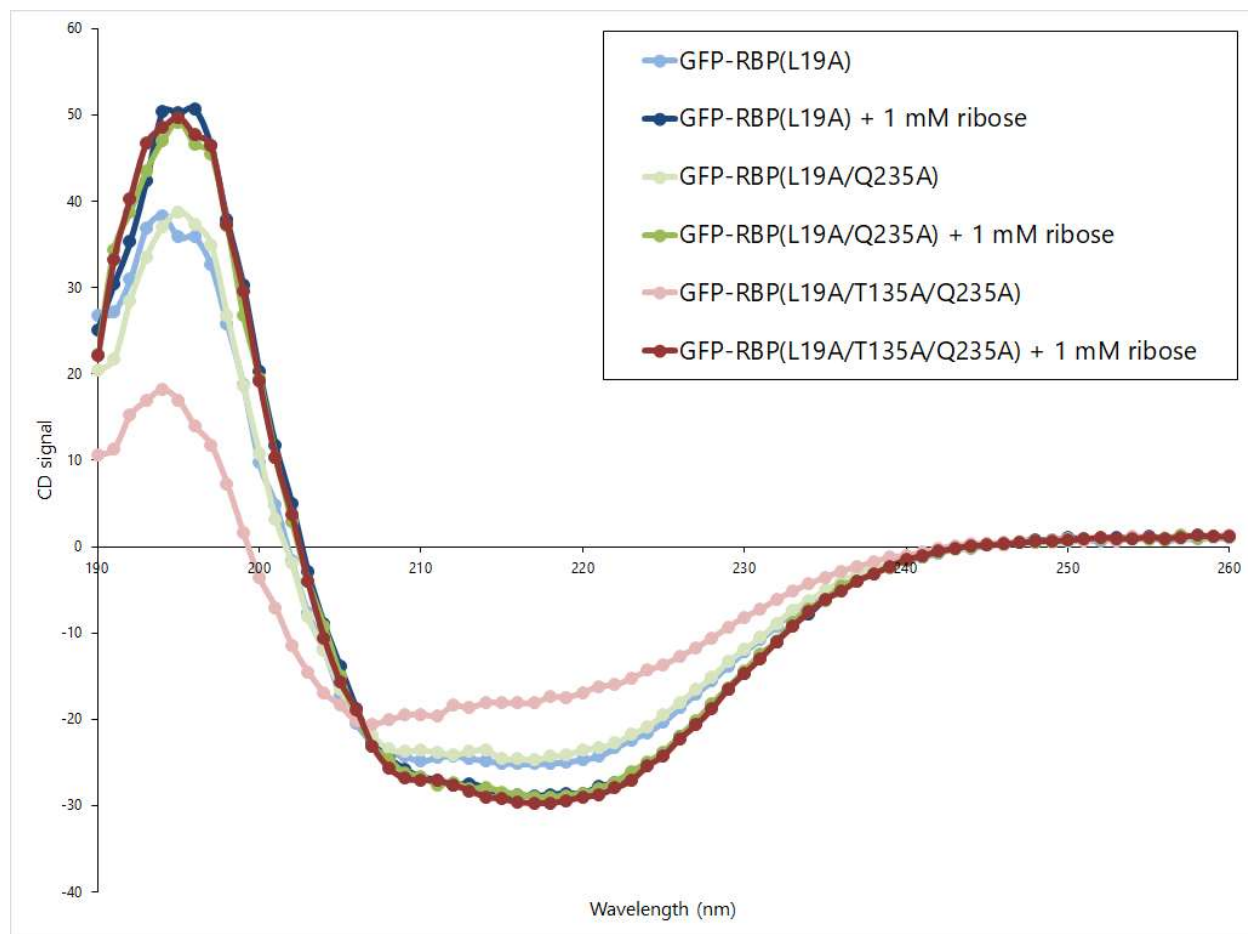


Figure S3. CD spectra of GFP-RBP(L19A) and mutants. Spectra taken from 5 μ M protein in 10 mM sodium phosphate buffer (pH 8.0) at 20 $^{\circ}$ C.

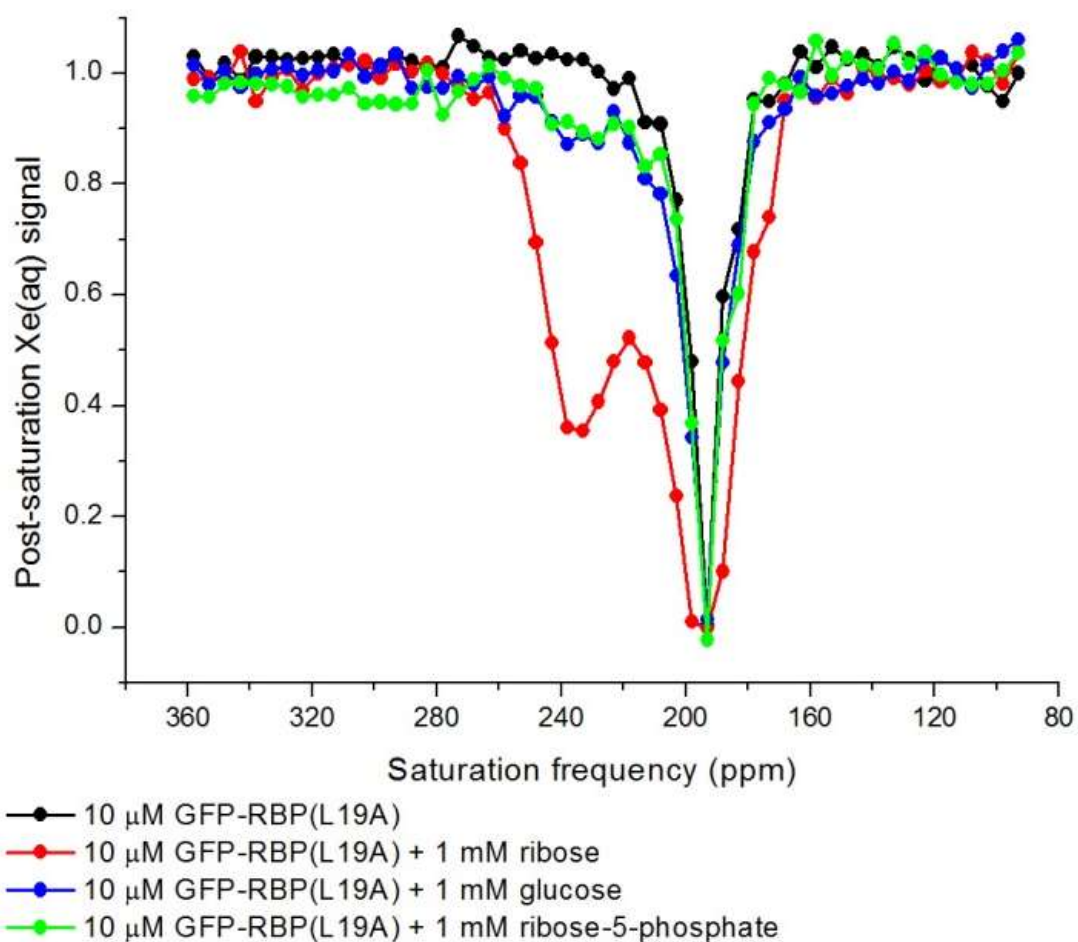


Figure S4. Hyper-CEST z-spectra of 10 μ M GFP-RBP(L19A) in PBS. Data acquired with protein in its unliganded state and in the presence of indicated ligands in pH 7.2 buffer at 300 K. Data shown as an average of 3 trials.

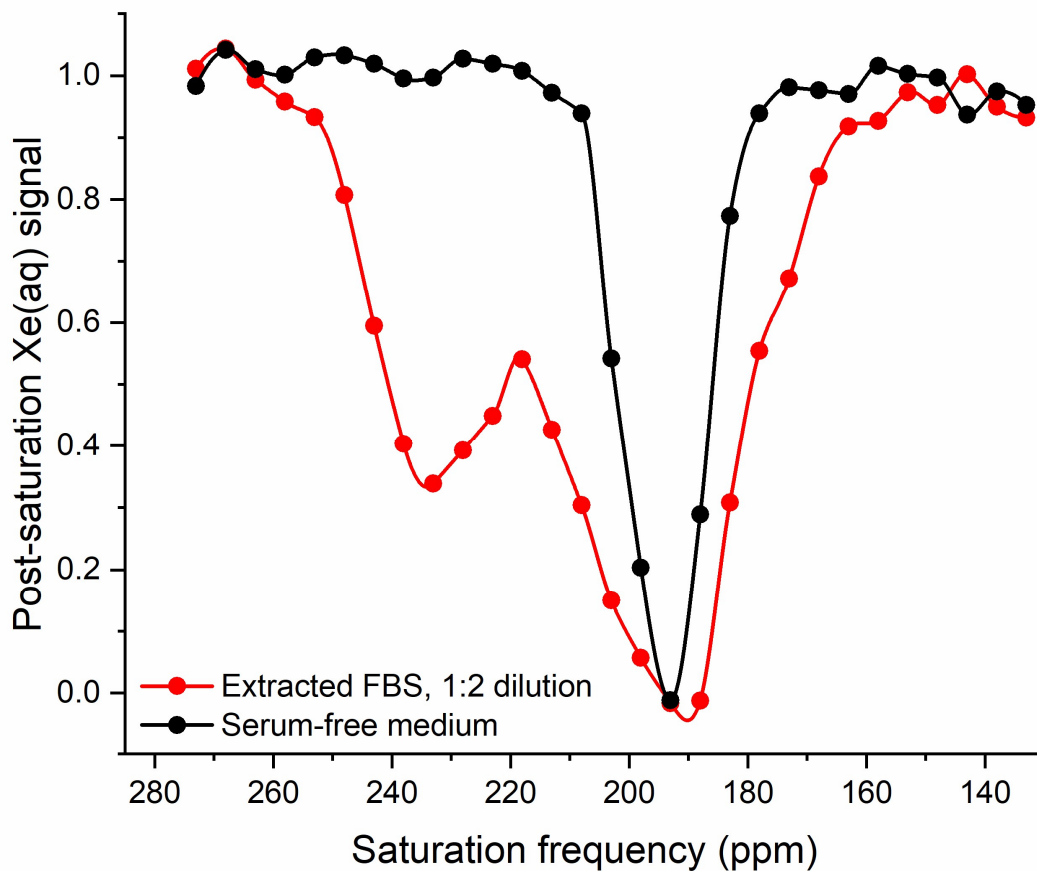


Figure S5. Hyper-CEST z-spectra of GFP-RBP(L19A) in FBS and serum-free medium. FBS was extracted with methanol following literature procedure¹ and then diluted 1:2 in PBS buffer. Pulse length, $\tau_{\text{pulse}} = 3.80$ ms; field strength, $B_{1,\text{max}} = 77$ μT . Experiments were performed at 300 K with 20 μM protein. Data shown as an average of 3 trials.

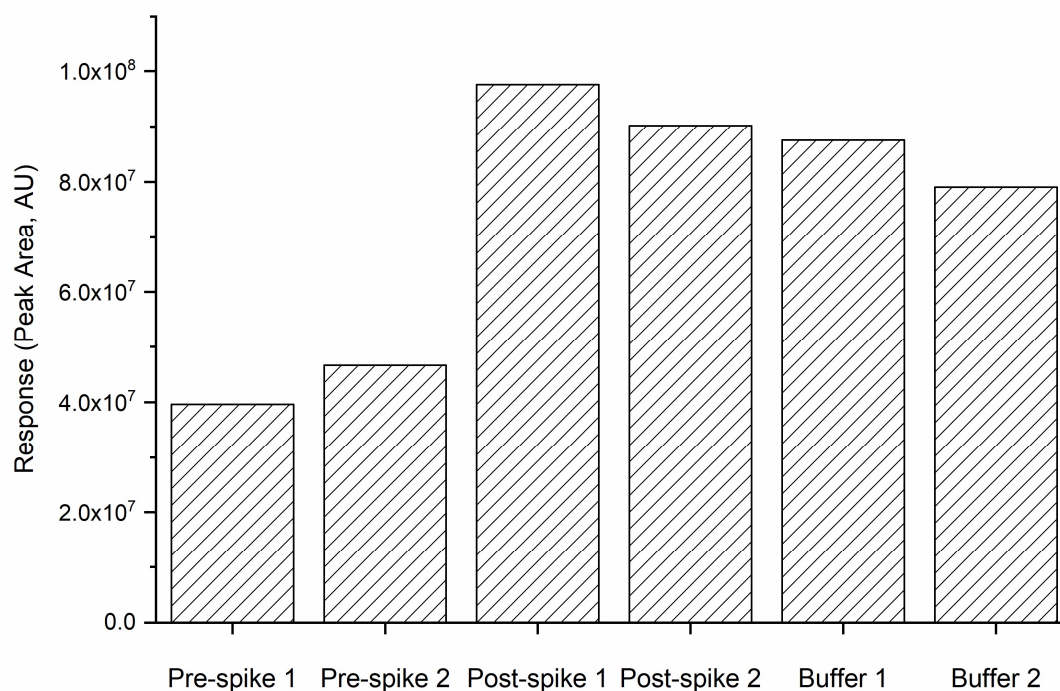


Figure S6. LC-MS response of [U-¹³C₅] ribose spiked into extracted HeLa cell lysate samples. “Pre-spike” corresponds to samples of 2 million/mL lysed HeLa cell extract spiked pre-extraction with [U-¹³C₅] ribose to a final concentration of 20 μM. “Post-spike” corresponds to samples of 2 million/mL lysed HeLa cell extract spiked post-extraction with [U-¹³C₅] ribose to a final concentration of 20 μM. “Buffer” corresponds to controls of the extraction solution only (1:2 ddH₂O:MeOH v/v) spiked with [U-¹³C₅] ribose to a final concentration of 20 μM. Each sample was injected twice. The acetate adduct peak was quantified. The peak areas for each sample are shown in Table S3.

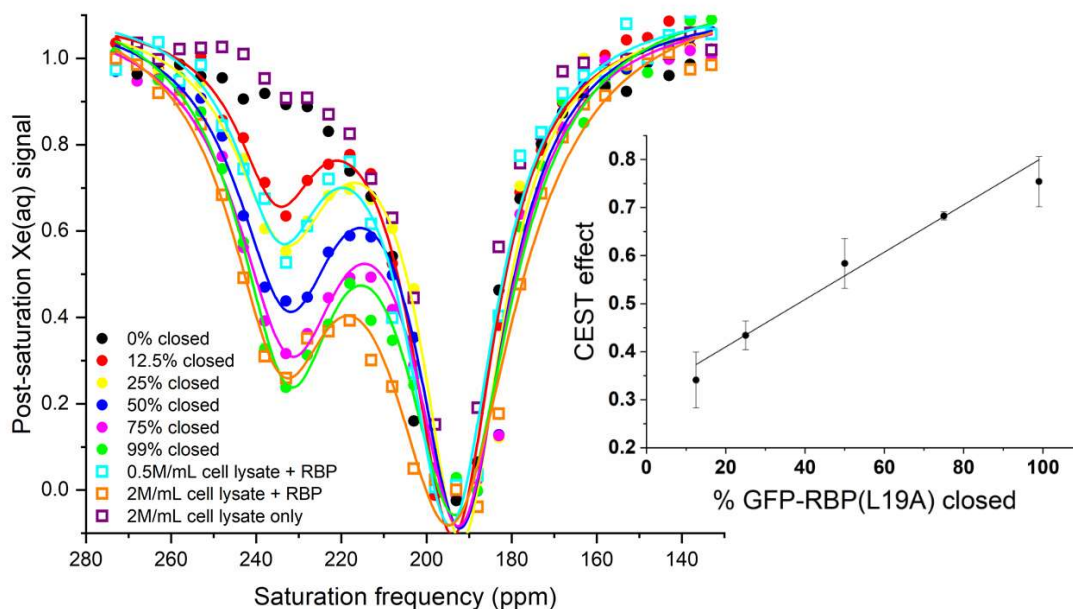


Figure S7. Hyper-CEST z-spectra of GFP-RBP(L19A) in FBS-supplemented HeLa cell lysate. Z-spectra of varying percentages of GFP-RBP(L19A) in the closed conformation ($[\text{ribose}] = 0, 2.5, 5.1, 10.3, 15.9, 49.5 \mu\text{M}$), and with cell lysate from HeLa cells grown in FBS-supplemented medium are shown. The z-spectrum of cell lysate only is shown for reference. All z-spectra were obtained with $20 \mu\text{M}$ GFP-RBP(L19A) in pH 7.2 PBS at 300 K. Pulse length, $\tau_{\text{pulse}} = 3.80 \text{ ms}$; field strength, $B_{1,\text{max}} = 77 \mu\text{T}$. Data shown as an average of 3 trials. Inset: the magnitude of the CEST effect from each z-spectrum plotted against the percentage of closed RBP. $R^2 = 0.982$.

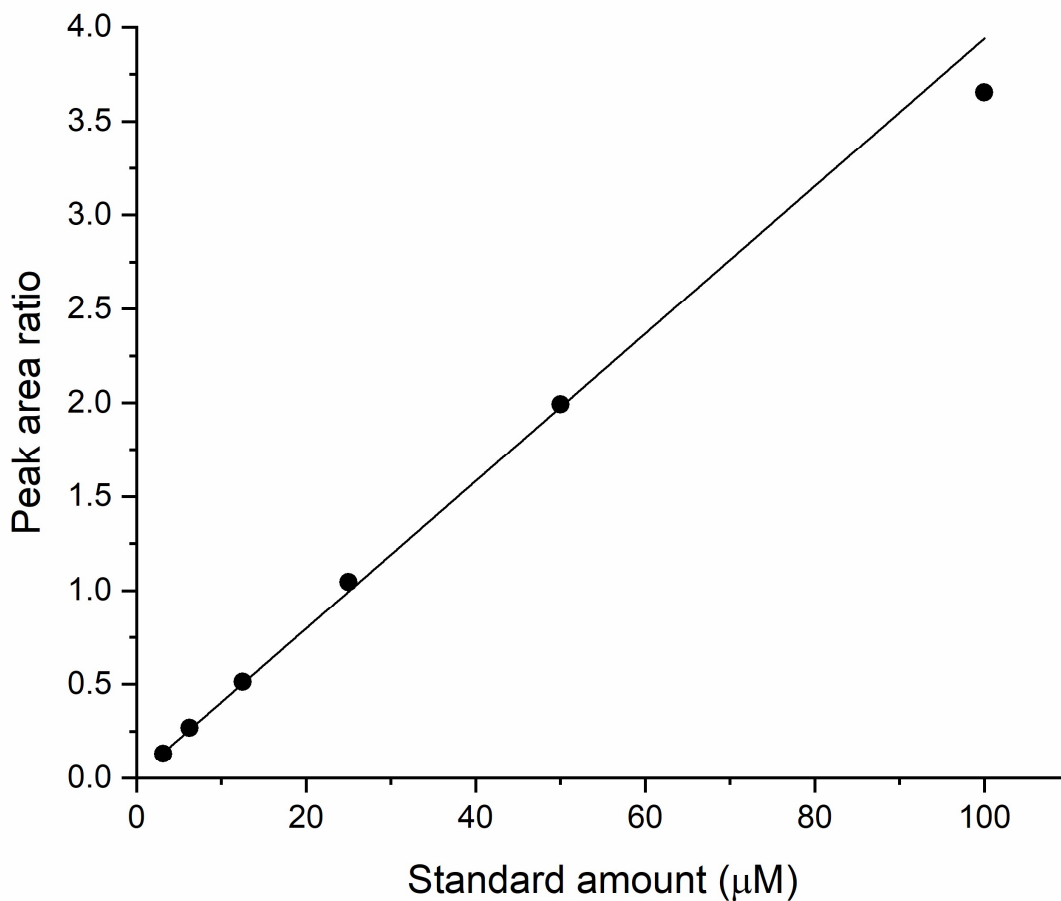


Figure S8. Ribose calibration curve for LC-MS analysis. Ribose was quantified as the ratio of the ribose standard peak area to the [U-¹³C₅] ribose internal standard peak area. The ribose standard concentrations used were 3.13, 6.25, 12.5, 25, 50, and 100 µM, with 20 µM [U-¹³C₅] ribose internal standard. $R^2 = 0.995$, slope = 0.0393 ± 0.001 , y-intercept = 0.0121 ± 0.008 . The acetate adduct peak was quantified. The peak areas for each sample are shown in Table S3.

Table S3. Peak areas and calculated ribose concentrations from LC-MS analysis.^a

	3.13 μM ribose	6.25 μM ribose	12.5 μM ribose	25 μM ribose	50 μM ribose	100 μM ribose	Pre- spike 1	Pre- spike 2	Post- spike 1	Post- spike 2	Buffer 1	Buffer 2
Ribose peak area	1.85 x 10^7	4.37 x 10^7	7.73 x 10^7	1.49 x 10^8	2.73 x 10^8	4.73 x 10^8	6.39 x 10^7	6.75 x 10^7	6.23 x 10^7	6.27 x 10^7	N/F	N/F
[U- ¹³ C ₅] ribose peak area	1.41 x 10^8	1.63 x 10^8	1.51 x 10^8	1.42 x 10^8	1.37 x 10^8	1.29 x 10^8	3.96 x 10^7	4.67 x 10^7	9.76 x 10^7	9.02 x 10^7	8.75 x 10^7	7.90 x 10^7
Light/ heavy ratio	0.13	0.27	0.51	1.05	1.99	3.66	1.61	1.45	0.64	0.70	N/A	N/A
Calculated ribose (μM)	3.02	6.54	12.7	26.3	50.4	92.7	40.7	36.5	15.9	17.4	N/A	N/A

^aAll samples spiked with [U-¹³C₅] ribose to a final concentration of 20 μM . The “pre-spike”, “post-spike”, and “buffer” terms refer to the same conditions as described in Figure S6. The acetate adduct peak was quantified.

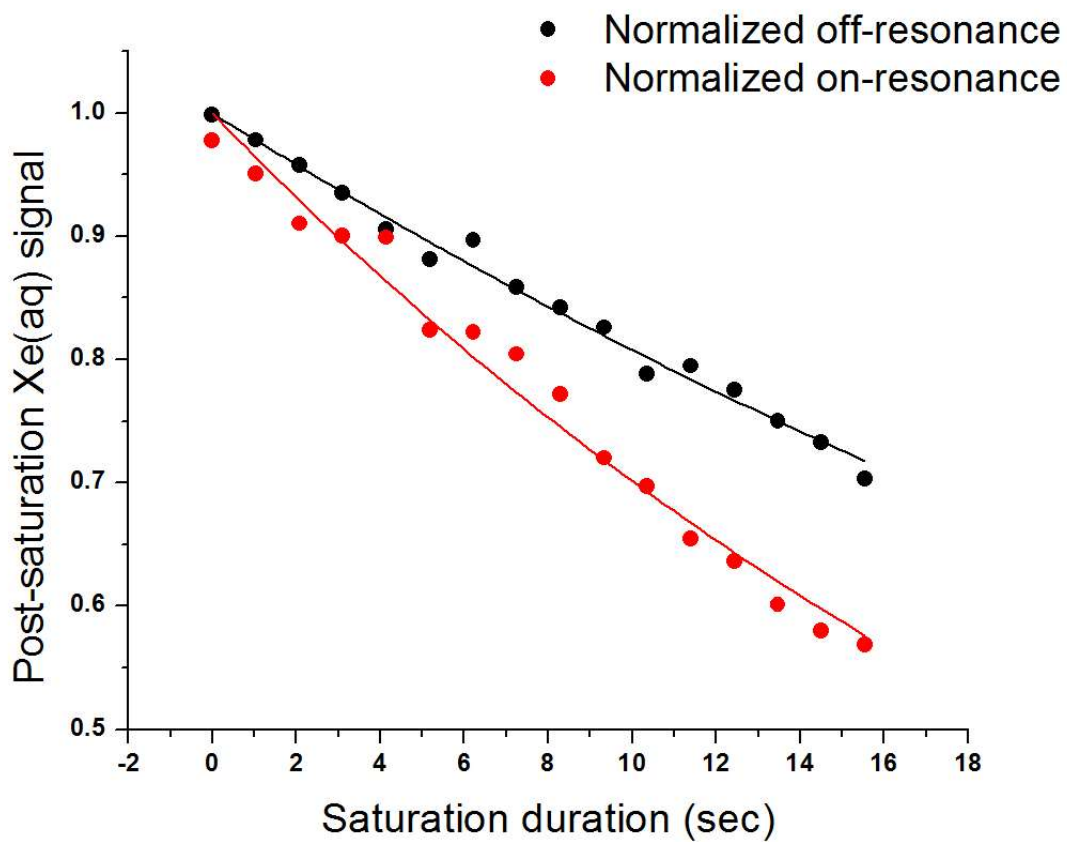


Figure S9. Time dependent saturation curves with GFP-RBP(L19A). Saturation contrast for 100 nM GFP-RBP(L19A) with 1 mM ribose at 300 K in pH 7.2 PBS buffer was determined to be 0.30 ± 0.01 . $T_{1\text{on}} = 28 \pm 1$ s and $T_{1\text{off}} = 47 \pm 1$ s. Pulse length, $\tau_{\text{pulse}} = 1.727$ ms; field strength, $B_{1,\text{max}} = 170$ μT . Data shown as an average of three trials.

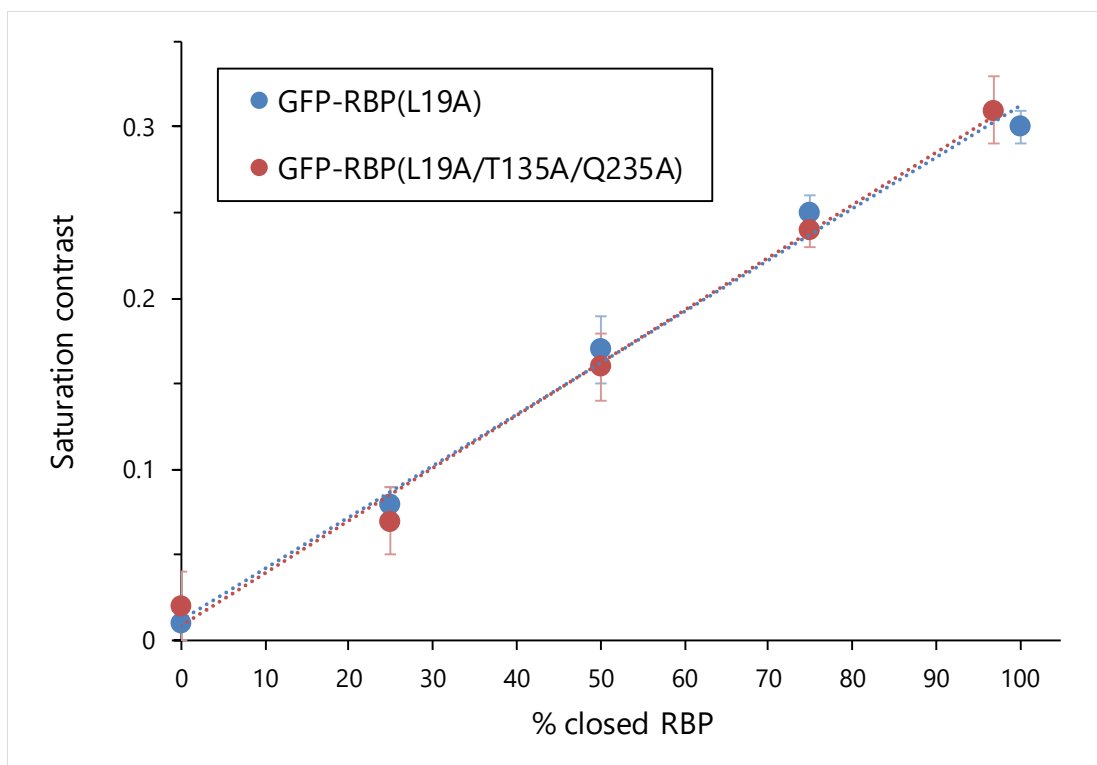


Figure S10. Saturation contrast as a function of ribose-bound RBP. Saturation contrast for 100 nM GFP-RBP(L19A) and 100 nM GFP-RBP(L19A/T135A/Q235A) at 300 K in pH 7.2 PBS buffer as a function of percent protein in the ribose-bound, closed conformation. For GFP-RBP(L19A), ($K_d = 0.3 \mu\text{M}$) [ribose] = 0, 0.15, 0.35, 0.975, 1000 μM . For GFP-RBP(L19A/T135A/Q235A), ($K_d = 130 \mu\text{M}$) [ribose] = 0, 43, 130, 390, 4000 μM . Pulse length, $\tau_{\text{pulse}} = 1.727 \text{ ms}$; field strength, $B_{1,\text{max}} = 170 \mu\text{T}$. Data shown as an average of three trials. Linear regressions for both sets of data reported R^2 values > 0.99 .

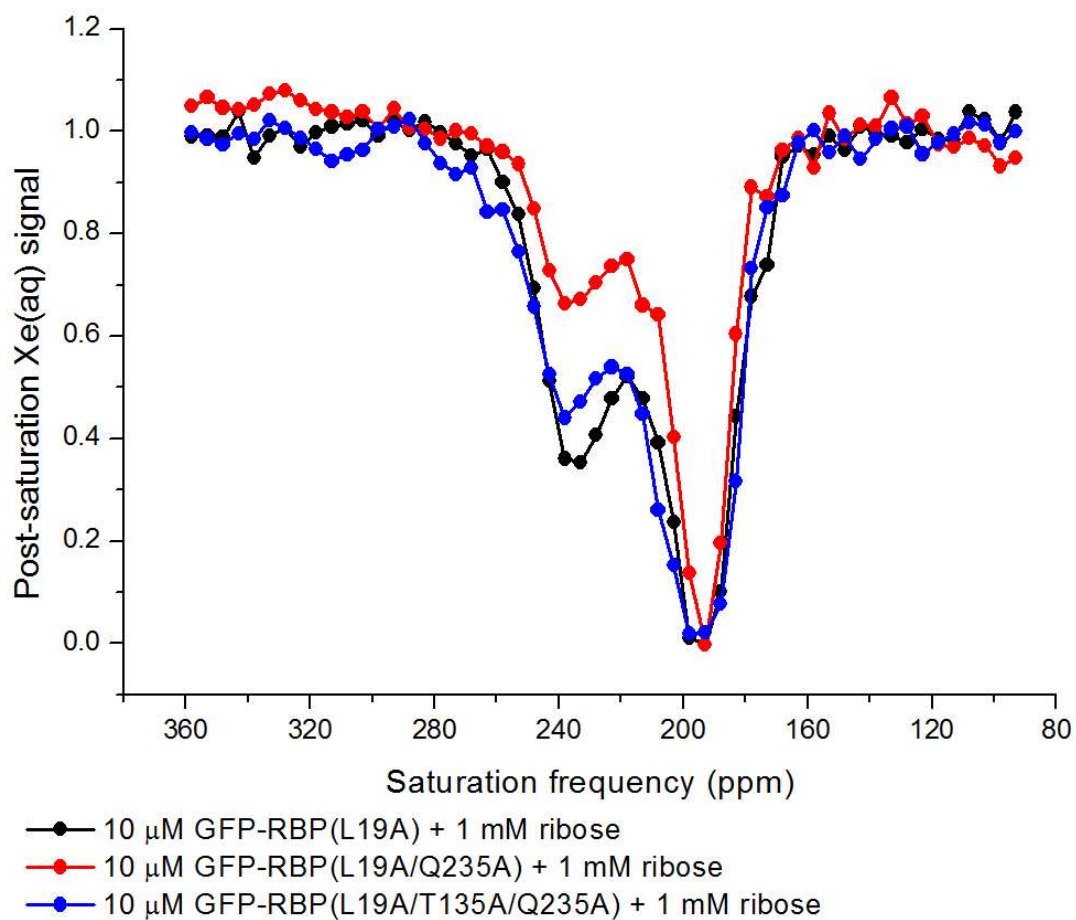


Figure S11. Hyper-CEST z-spectra of RBP mutants. Data acquired in pH 7.2 PBS at 300 K. Pulse length, $\tau_{\text{pulse}} = 3.80$ ms; field strength, $B_{1,\text{max}} = 77$ μ T. Data shown as an average of 3 trials.

References

- (1) Nagana Gowda, G. A.; Djukovic, D.; Bettcher, L. F.; Gu, H.; Raftery, D. *Anal. Chem.* **2018**, *90* (3), 2001–2009.